Loss of zinc finger homeobox-3 (ZFHX3) affects rhythmic gene transcription in mammalian central clock

Akanksha Bafna[1*], Gareth Banks[1], Patrick M. Nolan[1*]

[1]Medical Research Council, Harwell Science Campus, United Kingdom

*Corresponding author: a.bafna@har.mrc.ac.uk, pmnolan10@gmail.com

ABSTRACT

The mammalian suprachiasmatic nucleus (SCN), situated in the ventral hypothalamus, directs daily cellular and physiological 24-hr rhythms across the body. Spatiotemporal gene transcription in the SCN is vital for daily timekeeping to sustain the molecular circadian clock and clock-controlled genes (CCGs). A key SCN transcription factor, ZFHX3 (zinc finger homeobox-3), is implicated crucial for the synchronization and maintenance of the circadian timekeeping. So far, the resultant aberrant circadian behaviour after the loss of ZFHX3 is well-characterized, but the molecular mechanisms affecting the central clock, and the SCN transcriptome at large is poorly defined. Here, we used ZFHX3 targeted chromatin immunoprecipitation (ChIP-seq) to map the genomic localization of ZFHX3 in the SCN. In parallel, we conducted a comprehensive SCN RNA sequencing at six distinct times-of-day, and compared the transcriptional profile between the control and ZFHX3-conditional null mutants. Our rigorous efforts highlighted the genome wide occupancy of ZFHX3 predominantly around the gene transcription start site (TSS), co-localizing with the known histone modifications, and preferentially partnering with the core-clock TFs (CLOCK, BMAL1) to regulate the clock gene(s) transcription. We clearly showed a drastic effect of the loss of ZFHX3 on the SCN transcriptome, intensely reducing the level of neuropeptides

responsible for inter-cellular coupling, along with abolishing rhythmic (24-h) oscillation of the clock TF, *Bmal1*. A systematic rhythmicity analysis further showed change in phase (peak expression) and amplitude of the various clock genes including *Per (1-3)*, *Dbp* in ZFHX3 deficient mice, corroborating with the noted atypical advancement in daily behaviour under 12hr light- 12hr dark conditions. Taken together, these findings shed light on genome-wide regulation conferred by ZFHX3 in the central clock that is necessary to orchestrate daily timekeeping in mammals.

INTRODUCTION

Circadian (approximately one day) clocks is an internal biological clock, which enables molecular, behavioural and physiological processes to synchronize with changing daily environmental conditions and produce a coherent 24-hour rhythm. In mammals, the circadian clock mechanism consists of cell-autonomous transcription-translation feedback loops (TTFLs) that drive rhythmic, 24-h (hour) expression patterns of canonical clock components [1]. The first negative feedback loop is a rhythmic transcription of period genes (*Per1*, *Per2*, and *Per3*) and cryptochrome genes (*Cry1* and *Cry2*). PER and CRY proteins form a heterodimer, which acts on the CLOCK (circadian locomotor output cycles kaput) / BMAL1 (brain and muscle ARNT-Like 1) heterodimer to repress its own transcription. The second loop is a positive feedback loop driven by the CLOCK/BMAL1 heterodimer, which initiates transcription of target genes containing E-box cis-regulatory sequences.

The circadian processes are directed by suprachiasmatic nucleus (SCN) of the hypothalamus, which synchronizes robust 24-hour oscillations in peripheral tissues[2-4]. In the SCN, the TTFL drives the molecular clock in individual cells, which in turn are synchronized

through intercellular coupling and forms a coherent oscillator[5,6]. This intercellular coupling is driven by several neuropeptides, such as vasoactive intestinal peptide (VIP), arginine vasopressin (AVP) and gastrin-releasing peptide (GRP) [7], besides Prokinetin2 (PROK2) that serves as a pace making element in the SCN[8]. Along with the neuropeptides, a key zinc finger homeobox-3; ZFHX3, transcription factor is found to be highly prevalent in the discrete populations of the SCN cells, in adults, and shown to robustly control circadian rhythms. Intriguingly, while a dominant missense mutation in *Zfhx3* gene (short circuit, *Zfhx3*$^{Sci/+}$) causes mice to express a short circadian period [9], a complete conditional null *Zfhx3* mutation results in arrhythmicity [10]. Given the crucial role of the SCN in orchestrating daily timekeeping in mammals, it is imperative to fully understand the role of ZFHX3 in fine tuning the rhythmic processes.

Although the effect of *Zfhx3* mutation is known at the circadian behaviour level, the molecular defects underpinning perturbed daily timekeeping are not well-characterized. Therefore, we set out to systematically assess the functional significance of ZFHX3 by employing a multiomics approach in the SCN. Primarily, we focussed to analyse the genomic binding pattern of ZFHX3 in the central pacemaker by conducting ZFHX3 targeted chromatin immunoprecipitation (ChIP-seq). In parallel, we implemented a detailed transcriptional profiling of the *Zfhx3* conditional null mutants, specifically in the SCN using vibratome based microdissection[11], to infer the effect on tissue specific gene expression and rhythmic gene transcription. Overall, with our concerted efforts we are able to successfully pin-point genome-wide occupancy of ZFHX3 to specific gene regulatory regions in the SCN, potentially controlling vital SCN functions, including circadian timekeeping. Furthermore, our in-depth gene expression profiling has revealed a central role of *Zfhx3* in the SCN transcriptome, regulating various key tissue specific processes. Remarkably, we noted altered rhythmic transcriptional profile of the genes involved in the positive and negative loops of the

24-h driven feedback mechanisms at distinct levels in the ZFHX3-deficient mice, highlighting the importance of ZFHX3 in fine-tuning the molecular clockwork.

RESULTS

ZFHX3 binds to active promoter sites in the SCN

Genome-wide binding of transcription factor (TF) ZFHX3 was profiled in the suprachiasmatic nucleus (SCN) using chromatin immunoprecipitation (ChIP) sequencing. Briefly, genomic DNA was extracted from C57BL/6J mice raised in standard 12-h/12-h light-dark conditions at two distinct time-points; ZT3 and ZT15, and subjected to ChIP-Seq (Methods). The sequenced reads were aligned to mouse genome (mm10) and significant peaks corresponding to ZFHX3 occupancy were assessed in conjunction with previously identified histone modification regions[12] in the SCN. We noticed that majority of ZFHX3 peaks coincided with H3K4me3 and H3K27ac occupancy (48.9% of total ZFHX3 peaks at ZT3), and were focussed near the transcription start sites (TSS $\pm$ 3kb) (Fig. 1a,b). Presumably, these sites are responsible for active transcription as they are jointly occupied by H3K4me3 and H3K27ac [13], suggesting a potential role of ZFHX3 in regulating gene transcription in the SCN. On further inspection, the genes potentially regulated by ZFHX3 at the TSS were seen to be involved in synaptic processes and signalling pathways, including circadian timekeeping (Supplementary fig. 1a), which is a key function of the SCN.

On the other hand, genomic regions co-operatively bound by ZFHX3 and H3K4me3 (no H3K27ac, 20.7%), indicative of poised regulatory sites[14,15], or with ZFHX3 alone (22%) (Fig. 1d, e), were found to regulate genes involved in several fundamental biological processes, but not circadian rhythm (Supplementary fig. 1b, c). Therefore, it is plausible

ZFHX3 binds at the TSS and regulates actively transcribing genes, particularly those involved in tissue-specific functions such as daily timekeeping. This was further tested by examining the enrichment of DNA binding motifs at genomic sites occupied by ZFHX3 alone, and with specific histone modifications (H3K4me3, H3K27ac). As expected, we found overrepresentation of AT- rich known motifs at ZFHX3 sites[9], with ARNT(bHLH) domain enriched only where ZFHX3 peaks were seen adjacent to H3K27ac and H3K4me3 (active promoters). This clearly points towards the possibility of shared binding of ZFHX3 with the circadian clock TFs BMAL1/CLOCK at E-box (*CACGTG*) to regulate circadian gene transcription in the central pacemaker (Supplementary fig. 1d). Moreover, it is worth noting that CCCTC-binding factor (CTCF), known to attract both conserved and tissue-specific TFs [16,17], was also found to be enriched at ZFHX3 sites. Co-localization of CTCF with the SCN enriched transcription factor ZFHX3 could play an important role in chromatin organization and dynamic gene regulation, as seen previously in other tissues[18].

ZFHX3 knock-out (KO) invariably affects SCN transcriptomics

To study the role of ZFHX3 on the SCN transcriptome we employed total directional RNA sequencing on the SCN tissue collected from *Zfhx3*$^{Flox/Flox}$;UBC-Cre^{-} (Cre-neg) and *Zfhx3*$^{Flox/Flox}$;UBC-Cre^{+} (Pre-tam) , both serving as independent control groups, and tamoxifen administered *Zfhx3*$^{Flox/Flox}$;UBC-Cre^{+} (Post-tam) mutant group, at six distinct time-of-day (Methods). Alongside conducting RNA sequencing, we also measured the expression levels of *Zfhx3* by real-time PCR in control and mutant groups and found dramatic reduction in *Zfhx3* mRNA expression in the mutants (Supplementary fig. 2a). Overall, RNA sequencing revealed that 5,929 genes were affected in the SCN (FDR $\leq$ 0.05), with 2,878 downregulated and 3,051 upregulated post ZFHX3-KO (Supplementary table 1, Fig. 2a, b). As expected,

both the control groups (Cre-neg and Pre-tam) showed consistent differential gene expression levels when compared to the mutant and mitigated any downstream effect of tamoxifen dosing (Fig. 2b,c). We, then sub-selected highly differential genes ($\log_2$FC $\geq$1, FDR < 0.05) and conducted functional gene enrichment analysis. Consistent with the previous studies[9,10,19,20], genes that were downregulated were seen to be involved in neuropeptide signalling pathways (*Vip, Grp*), neuron differentiation, circadian rhythm etc., while those that were upregulated showed functional enrichment for cell differentiation and extracellular matrix organization processes. Interestingly, our comprehensive assessment also highlighted an effect of loss of ZFHX3 on the genes involved in learning and memory (*Grpr, Ghsr*), psychomotor behaviour (*Grp*), fear response and feeding behaviour (*Nmu*). Therefore, it is conceivable that loss of AT-motif binding ZFHX3 leads to drastic physiological impairment both at the tissue- and –system level in mammals.

Loss of Zfhx3 weakens the daily clock affecting rhythmic gene transcription at multiple levels

Recent studies investigating the circadian behaviour after the loss of ZFHX3, either due to a missense mutation (*Zfhx3*^{Sci}) [9] or knock-out (*Zfhx3*$^{Flox/Flox}$;UBC-Cre^{+}) [10], have successfully shown severe deficits in daily timekeeping resulting due to shortening of 24-h period (*tau = 23.0*) and arrhythmic locomotor activity, respectively. In order to further investigate the effect of ZFHX3 on the molecular circadian clock, we assessed the gene expression levels in the SCN at six distinct time-of-day[21], starting at zeitgeber time (ZT) = 2 for every 4 hours (Methods). In total, we analysed daily transcriptional profile of 24,421 genes in the SCN and compared the rhythmicity index between the control (Cre-neg) and mutant (Post-tam) groups using an R-based statistical framework *dryR* (https://github.com/naef-lab/dryR) [22].

Specifically, the analysed genes resulted into 5 distinct modules; module 1 referred to genes with no detected 24-h rhythm in their expression levels in both conditions (n = 16945, Supplementary fig. 3a), module 2 constituted genes that lost rhythmic expression after ZFHX3-KO (n =1630, fig. 3a), module 3 constituted genes that gain daily rhythmicity after ZFHX3-KO (n = 431, Supplementary fig. 3b), module 4 was composed of genes with no change in rhythmicity between the control and mutants (n = 1742, fig. 3b), and module 5 included genes that retain rhythmic expression with change in either amplitude or phase (peak expression) in the mutant group (n = 73) (Supplementary table 2, fig. 3c). For each module, we compiled the gene list and assayed the functional enrichment pathways. Interestingly, we found that almost all the canonical clock genes belonged to module 5, including *Per2*, and showed change in phase and/ amplitude.

Intriguingly, this systematic approach did not only highlighted the genes that lost 24-h rhythmic oscillations, such as *Bmal1* and the SCN neuropeptide *Avp* (module 2, fig. 3a), but also identified genes that retained rhythmicity with change in their waveform (module 5). Given the fact that ZFHX3 deficient mice do not lose rhythmic behaviour in daily LD cycle [10] (Supplementary fig. 2b), but results in arrhythmia in free-running (complete darkness: DD) condition, we believe our targeted SCN specific assessment shed light on the dynamics of the daily gene expression pattern linked to the knock-out condition. Although the clock genes did not lose rhythmic expression under LD condition, they all showed characteristic phase (peak expression) advance that perfectly corroborated with advancement in the locomotor activity (at onset of dark; ZT12), seen for the mutants. Therefore at the molecular level, loss of ZFHX3, results in loss of rhythmic gene expression of clock TF- such as *Bmal1* and phase advance for core-clock genes, with the exception of CRY family genes *(Cry1, Cry2)* that did not reveal any obvious change and resulted in module 4.

DISCUSSION

The SCN is distinctive in its ability to sustain autonomous rhythmicity which is driven by circadian cascades of transcription that direct metabolic, electrophysiological and signalling rhythms. Our current finding highlights the instrumental role of transcription factor, ZFHX3 in driving the daily timekeeping mechanism. Through the targeted ChIP-seq we pinpointed the genome-wide occupancy of ZFHX3 in the SCN, which was found to be co-localized with histone modifications (H3K4me3, H3K27ac) and concentrated near the gene TSS. That said, a vast majority of ZFHX3 sites were also seen at distal intergenic regions (Fig. 1c, e), devoid of the promoter histone methylation mark, and enriched for CTCF binding sites. This hints on the potential accessory role of ZFHX3 in modifying genome topology and chromosomal looping to bring about change in target gene expression by regulating the promoter-enhancer interactions[23]. Interestingly, along with the CTCF binding sites, ZFHX3 bound sites were also enriched for other SCN domineering regulatory factors; RFX, LHX, ZIC [24,25] (Supplementary fig. 1d), suggesting a well-coordinated tissue-specific gene regulation.

Next, given the crucial role of ZFHX3 in daily timekeeping, we speculated a dynamic change in its genomic occupancy and compared the binding intensity of the transcription factor at two anti-phasic (12-h apart, zt3 vs zt15) time-points (Methods). Surprisingly, we did not detect any differential binding site(s) between the tested time-points, but rather noticed a uniform and coherent localization. This suggests towards ZFHX3 belonging to a family of poised transcription factors, who either could act as a co-activator/mediator to regulate the target gene transcription or responsible for chromatin accessibility. Indeed, in a recent unpublished study by Baca et al[26], ZFHX3 was shown to be associated with chromatin remodelling and mRNA processing. Nonetheless, in our study we clearly noted ZFHX3 bound active TSS to be enriched for BMAL1 binding site (CACGTG) that could clearly explain the control of circadian gene transcription by ZFHX3.

Along with the ChIP-seq, we executed a detailed RNA sequencing to study the effect of loss of ZFHX3, particularly in the SCN. Crucially, ZFHX3 affected the SCN transcriptome at varied levels, to an extent where advancement in rhythmic behaviour is resonated in the resultant altered amplitude/phase (peak expression) of canonical clock genes in ZFHX3 deficient mice under 12-h light and 12-h dark (daily) conditions. Broadly speaking, the majority of clock genes did not lose 24-h rhythmicity *(as Bmal1)*, but showed an even early peak in expression, ranging between ~0.4 – 2 hours. It is, however, noteworthy that the CRY family of genes *(Cry1, Cry2)* did not show the advancement in expression levels, and is supposedly shielding the molecular clock as shown by Abe et al[27]. In fact, loss of rhythmic *Bmal1* gene transcription after ZFHX3-KO cannot be assumed to functionally abolish BMAL1 oscillation, which has been shown to sustain due to post-translation regulation [23], and could explain the subsequent 24-h driven *Per(1,2,3)* and *Cry(1,2)* mRNA rhythms. On the other hand, the noted change in amplitude (decreased) and phase shed light on the exclusive interaction between ZFHX3 and affected clock genes in the SCN. Regardless, ZFHX3 exerts an imperative control on the clock gene transcription which in turn controls the daily behavioural rhythm, as seen in this study.

.

METHODS

Mice

All animal studies were performed under the guidance issued by Medical Research Council in Responsibility in the Use of Animals for Medical Research (July1993) and Home Office Project Licence 19/0004. Adult specific knock out *Zfhx3* mice were generated using an inducible Cre line as described by Wilcox et al[10]. Briefly, tamoxifen inducible Cre mice (UBC-Cre) were crossed to *Zfhx3* floxed (*Zfhx3*^{Flox}) mice to produce an initial stock of

Zfhx3$^{Flox/+}$;UBC-Cre^{+} mice. These were subsequently crossed to *Zfhx3*$^{Flox/+}$ mice to generate experimental cohorts [28]. Out of the 6 possible genotype combinations, 2 genotypes; *Zfhx3*$^{Flox/Flox}$;UBC-Cre^{-} (mice homozygous for *Zfhx3*^{Flox} allele but not carrying the Cre allele) and *Zfhx3*$^{Flox/Flox}$;UBC-Cre^{+} (mice homozygous for *Zfhx3*^{Flox} allele and hemizygous for Cre allele) were assigned as "control" (Cre-neg) and "experimental" (Post-tam) groups, respectively and dosed with tamoxifen. In addition, we also included a cohort of *Zfhx3*$^{Flox/Flox}$;UBC-Cre^{+} mice before tamoxifen treatment as a secondary control (Pre-tam). Animals were group housed (4-5 mice per age) in individually ventilated cages under 12:12hr light-dark conditions with food and water available ad libitum.

Experimental Design

Mice (aged between 8 to 12 weeks) from control (Cre-neg and Pre-tam) and *Zfhx3* knock out (Post-tam) cohorts were used for SCN tissue collection at 6 distinct time-points starting from ZT2 at every 4 hours, where lights on at 7 am (ZT0) and lights off at 7 pm (ZT12). For SCN RNA-Seq, four biological replicates per time-point were collected independently from the control and experimental groups. For the second control group viz. Pre-tam; 2-4 biological replicates were collected due to time constraints. Furthermore, each biological replicate for all the three tested condition constituted 3 individual SCN samples.

SCN tissue collection

Animals were sacrificed at the aforementioned time-points by cervical dislocation and brains were removed and flash frozen on dry ice. The frozen brains were placed on dry ice along with the brain matrix (Kent Scientific, Torrington CT, USA) and razor blades to chill. The brain dissection was performed on a vibrating microtome (7000smz-2 Vibrotome, Campden Instruments) under chilled conditions [11]. First, the frozen brain was placed on the chilled brain matrix and ca. 3mm thick region was removed using razor blade from the caudal end to

remove the cerebellum and attain flat surface. Then, the dissected brain was super-glued to a chilled (2 –3°C) metal chuck and placed into the metal specimen tray of the Vibratome. The metal specimen tray was filled with pre-chilled 1X RNase free PBS (phosphate buffered saline, ThermoFisher Scientific, #AM9625). Coronal slices measuring 250 uM in thickness were cut from rostral to caudal at slow speed (0.07mm/s) and pre-tested specifications ; Frequency: 70Hz, Amplitude: 1.00mm. Once cut, the slice with intact optic chiasm, third ventricle and bilateral SCN tissues (Fig. S1) was selected and transferred on to pre-chilled glass slides (ThermoFisher Scientific SuperFrost Plus Adhesion slides) with the help of paint brush. The glass slide was placed on top of cold block and SCN tissues were collected by pre-chilled forceps and dissection needles under dissection microscope (Nikon SMZ645 Stereo Microscope).

RNA extraction

Total RNA from each sample replicate was extracted using RNeasy Micro Kit (QIAGEN, #74004) following the protocol for microdissected cryosections as per manufacturer's guidelines and stored at -80°C. Quality and quantity of RNA were measured using an Agilent Bioanalyzer (Pico chip) and a Nanodrop1000 (Thermo Fisher Scientific, Waltham, MA USA), respectively.

RNA Sequencing and data analysis

PolyA RNA-Seq libraries were prepared by Oxford Genomics Centre, University of Oxford using NEBNext Ultra II Directional RNA Library Prep Kit (NEB, #E7760) and sequenced on NovaSeq6000_150PE (150 bp paired-end directional reads: ~40 million reads/sample) platform. Paired-end FASTQ files were quality assessed (Phred<20 removed) with FastQC and Illumina adapters were trimmed with TrimGalore (v0.4.3). Then, the reads were aligned to mm10 genome assembly using STAR (v2.7.8a) with MAPQ value for unique mappers set

to 60. Binary alignment map (BAM) files were used to generate read counts per gene by FeatureCounts via Samtools (v1.11). Finally, limma-voom method (Liu et al. 2015) from the Bioconductor package-limma (v3.48.0) was adopted to quantify differential gene expression and normalised logarithmic CPM values were generated for downstream analysis.

Differential rhythm analysis

The read counts per gene for each analysed sample was obtained by FeatureCounts and arranged in sample matrix by using coreutils (v8.25). The matrix file was used as an input for *dryR* (R package for Differential Rhythmicity Analysis) available at https://github.com/neaf-lab/dryR . Normalized transcripts from "control" (Cre-neg) and "experimental" (Post-tam) groups were categorized into 5 modules with a threshold of BICW (Bayes information criterion weight) > 0.4 based on their time-resolved expression pattern.

Gene annotation

The gene list were derived from Bioconductor-based package ChIPseeker v1.28.3 [29] was fed into the Database for Annotation, Visualization, and Integrated Discovery (DAVID) tool [30]. The functional annotation chart based on KEGG pathway, Gene Ontology (GO): biological processes (BP) was plotted with the help of the ggplot2 package in Rv4.0.5 (https://ggplot2.tidyverse.org/).

HOMER motif analysis

The findMotifsGenome.pl function within the HOMER v4.11 package [31] was used to identify enriched motifs and their corresponding TFs with options size 200 –len 8, 10, 12 –mask –preparse –dumpfasta, with default background regions.

FUNDING

PMN and AB were supported by Medical Research Council (MC_U142684173). GB was supported by the UK Dementia Research Institute which receives its funding from DRI Ltd., funded by the UK Medical Research Council, Alzheimer's Society and Alzheimer's Research United Kingdom.

AUTHOR CONTRIBUTION

AB, GB and PMN conceived the study. AB and GB were involved in sample collection and processing. AB and PMN carried out the investigation with AB conducting the formal data analysis. Data visualization was performed by AB, GB and PMN. Supervision of the research was carried out by PMN. The original draft was written by AB. Manuscript was reviewed, edited and finalised by AB, GB and PMN.

COMPETING INTERESTS

Authors declare that they have no competing interests.

ACKNOWLEDGEMENTS

We thank the staff of the Mary Lyon Centre and core services at MRC Harwell Institute for assistance with mouse studies. We thank Dr Benjamin Weger, University of Queensland for his valuable suggestions and timely inputs during data analysis. We also thank Richard Reeves for data accessibility on UCSC genome browser. This research was supported by the Medical Research Council (MC_U142684173) grant to PMN.

REFERENCES

313 1 Takahashi, J. S., Hong, H. K., Ko, C. H. & McDearmon, E. L. The genetics of mammalian
314 circadian order and disorder: implications for physiology and disease. *Nat Rev Genet* **9**, 764-
315 775 (2008). https://doi.org/10.1038/nrg2430
316 2 Schibler, U. *et al.* Clock-Talk: Interactions between Central and Peripheral Circadian
317 Oscillators in Mammals. *Cold Spring Harb Symp Quant Biol* **80**, 223-232 (2015).
318 https://doi.org/10.1101/sqb.2015.80.027490
319 3 Hastings, M. H., Maywood, E. S. & Brancaccio, M. Generation of circadian rhythms in the
320 suprachiasmatic nucleus. *Nat Rev Neurosci* **19**, 453-469 (2018).
321 https://doi.org/10.1038/s41583-018-0026-z
322 4 Hastings, M. H., Maywood, E. S. & Brancaccio, M. The Mammalian Circadian Timing System
323 and the Suprachiasmatic Nucleus as Its Pacemaker. *Biology (Basel)* **8** (2019).
324 https://doi.org/10.3390/biology8010013
325 5 Herzog, E. D., Hermanstyne, T., Smyllie, N. J. & Hastings, M. H. Regulating the
326 Suprachiasmatic Nucleus (SCN) Circadian Clockwork: Interplay between Cell-Autonomous
327 and Circuit-Level Mechanisms. *Cold Spring Harb Perspect Biol* **9** (2017).
328 https://doi.org/10.1101/cshperspect.a027706
329 6 Maywood, E. S., Chesham, J. E., Winsky-Sommerer, R. & Hastings, M. H. Restoring the
330 Molecular Clockwork within the Suprachiasmatic Hypothalamus of an Otherwise Clockless
331 Mouse Enables Circadian Phasing and Stabilization of Sleep-Wake Cycles and Reverses
332 Memory Deficits. *J Neurosci* **41**, 8562-8576 (2021).
333 https://doi.org/10.1523/JNEUROSCI.3141-20.2021
334 7 Brown, T. M., Hughes, A. T. & Piggins, H. D. Gastrin-releasing peptide promotes
335 suprachiasmatic nuclei cellular rhythmicity in the absence of vasoactive intestinal
336 polypeptide-VPAC2 receptor signaling. *J Neurosci* **25**, 11155-11164 (2005).
337 https://doi.org/10.1523/JNEUROSCI.3821-05.2005
338 8 Morris, E. L. *et al.* Single-cell transcriptomics of suprachiasmatic nuclei reveal a Prokineticin-
339 driven circadian network. *EMBO J* **40**, e108614 (2021).
340 https://doi.org/10.15252/embj.2021108614
341 9 Parsons, M. J. *et al.* The Regulatory Factor ZFHX3 Modifies Circadian Function in SCN via an
342 AT Motif-Driven Axis. *Cell* **162**, 607-621 (2015). https://doi.org/10.1016/j.cell.2015.06.060
343 10 Wilcox, A. G., Vizor, L., Parsons, M. J., Banks, G. & Nolan, P. M. Inducible Knockout of Mouse
344 Zfhx3 Emphasizes Its Key Role in Setting the Pace and Amplitude of the Adult Circadian
345 Clock. *J Biol Rhythms* **32**, 433-443 (2017). https://doi.org/10.1177/0748730417722631
346 11 Bafna, A., Lau, P., Banks, G. & Nolan, P. M. Harvesting mouse suprachiasmatic nucleus by
347 vibrating microtome for diurnal transcriptome analysis. *STAR Protoc* **4**, 102618 (2023).
348 https://doi.org/10.1016/j.xpro.2023.102618
349 12 Bafna, A., Banks, G., Hastings, M. H. & Nolan, P. M. Dynamic modulation of genomic
350 enhancer elements in the suprachiasmatic nucleus, the site of the mammalian circadian
351 clock. *Genome Res* **33**, 673-688 (2023). https://doi.org/10.1101/gr.277581.122
352 13 Beacon, T. H. *et al.* The dynamic broad epigenetic (H3K4me3, H3K27ac) domain as a mark of
353 essential genes. *Clin Epigenetics* **13**, 138 (2021). https://doi.org/10.1186/s13148-021-01126-
354 1
355 14 Calo, E. & Wysocka, J. Modification of enhancer chromatin: what, how, and why? *Mol Cell*
356 **49**, 825-837 (2013). https://doi.org/10.1016/j.molcel.2013.01.038
357 15 Creyghton, M. P. *et al.* Histone H3K27ac separates active from poised enhancers and
358 predicts developmental state. *Proc Natl Acad Sci U S A* **107**, 21931-21936 (2010).
359 https://doi.org/10.1073/pnas.1016071107
360 16 Holwerda, S. J. & de Laat, W. CTCF: the protein, the binding partners, the binding sites and
361 their chromatin loops. *Philos Trans R Soc Lond B Biol Sci* **368**, 20120369 (2013).
362 https://doi.org/10.1098/rstb.2012.0369

363 17 Xu, Y. *et al.* Long-Range Chromosome Interactions Mediated by Cohesin Shape Circadian
364 Gene Expression. *PLoS Genet* **12**, e1005992 (2016).
365 https://doi.org/10.1371/journal.pgen.1005992
366 18 Qi, Q. *et al.* Dynamic CTCF binding directly mediates interactions among cis-regulatory
367 elements essential for hematopoiesis. *Blood* **137**, 1327-1339 (2021).
368 https://doi.org/10.1182/blood.2020005780
369 19 Hughes, S. *et al.* Zfhx3 modulates retinal sensitivity and circadian responses to light. *FASEB J*
370 **35**, e21802 (2021). https://doi.org/10.1096/fj.202100563R
371 20 Wilcox, A. G. *et al.* Zfhx3-mediated genetic ablation of the SCN abolishes light entrainable
372 circadian activity while sparing food anticipatory activity. *iScience* **24**, 103142 (2021).
373 https://doi.org/10.1016/j.isci.2021.103142
374 21 Hughes, M. E. *et al.* Guidelines for Genome-Scale Analysis of Biological Rhythms. *J Biol*
375 *Rhythms* **32**, 380-393 (2017). https://doi.org/10.1177/0748730417728663
376 22 Weger, B. D. *et al.* Systematic analysis of differential rhythmic liver gene expression
377 mediated by the circadian clock and feeding rhythms. *Proc Natl Acad Sci U S A* **118** (2021).
378 https://doi.org/10.1073/pnas.2015803118
379 23 Pugacheva, E. M. *et al.* CTCF mediates chromatin looping via N-terminal domain-dependent
380 cohesin retention. *Proc Natl Acad Sci U S A* **117**, 2020-2031 (2020).
381 https://doi.org/10.1073/pnas.1911708117
382 24 Araki, R. *et al.* Restricted expression and photic induction of a novel mouse regulatory factor
383 X4 transcript in the suprachiasmatic nucleus. *J Biol Chem* **279**, 10237-10242 (2004).
384 https://doi.org/10.1074/jbc.M312761200
385 25 Hatori, M. *et al.* Lhx1 maintains synchrony among circadian oscillator neurons of the SCN.
386 *Elife* **3**, e03357 (2014). https://doi.org/10.7554/eLife.03357
387 26 Del Rocío Pérez Baca, M. *et al.* A novel neurodevelopmental syndrome caused by loss-of-
388 function of the Zinc Finger Homeobox 3 (ZFHX3) gene. *medRxiv* (2023).
389 https://doi.org/10.1101/2023.05.22.23289895
390 27 Abe, Y. O. *et al.* Rhythmic transcription of Bmal1 stabilizes the circadian timekeeping system
391 in mammals. *Nat Commun* **13**, 4652 (2022). https://doi.org/10.1038/s41467-022-32326-9
392 28 Sun, X. *et al.* Heterozygous deletion of Atbf1 by the Cre-loxP system in mice causes
393 preweaning mortality. *Genesis* **50**, 819-827 (2012). https://doi.org/10.1002/dvg.22041
394 29 Yu, G., Wang, L. G. & He, Q. Y. ChIPseeker: an R/Bioconductor package for ChIP peak
395 annotation, comparison and visualization. *Bioinformatics* **31**, 2382-2383 (2015).
396 https://doi.org/10.1093/bioinformatics/btv145
397 30 Dennis, G. *et al.* DAVID: Database for Annotation, Visualization, and Integrated Discovery.
398 *Genome Biol* **4**, P3 (2003).
399 31 Heinz, S. *et al.* Simple combinations of lineage-determining transcription factors prime cis-
400 regulatory elements required for macrophage and B cell identities. *Mol Cell* **38**, 576-589
401 (2010). https://doi.org/10.1016/j.molcel.2010.05.004

402

Figure 1

A

Overlap of ZFHX3 binding with histone modifications

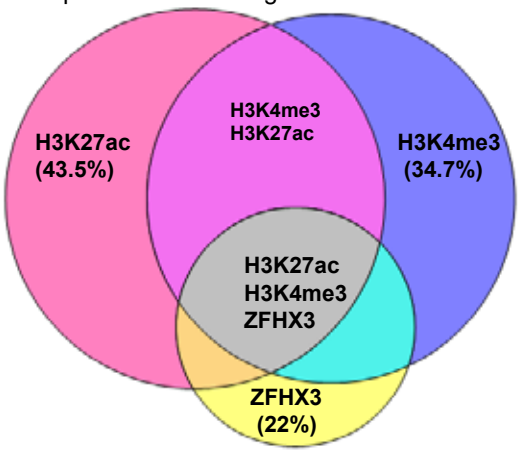

Category	Number of sites
Only H3K27ac	47552
Only H3K4me3	35673
Only ZFHX3	9512
H3K4me3 + ZFHX3	8992
H3K27ac + ZFHX3	3570
H3K27ac + H3K4me3	36819
H3K27ac + H3K4me3 + ZFHX3	21162

B H3K27ac+H3K4me3+ZFHX3

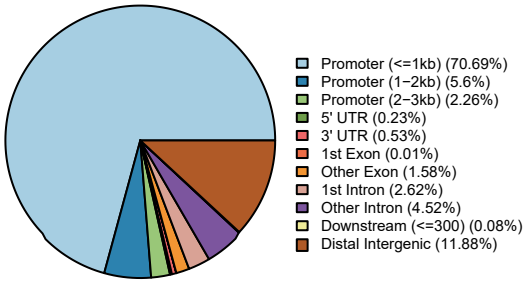

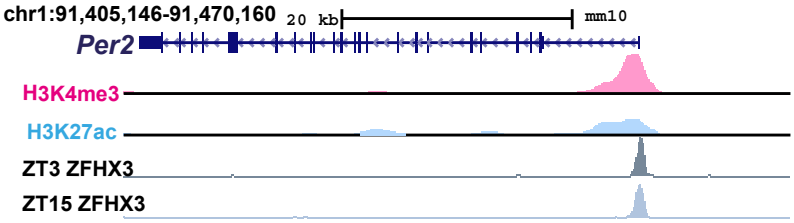

C H3K27ac+ZFHX3

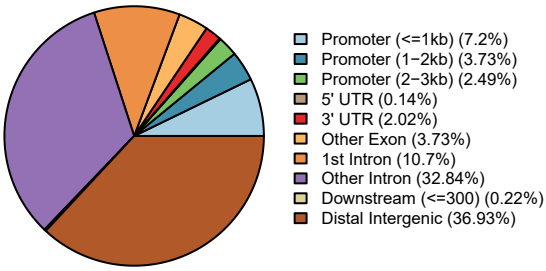

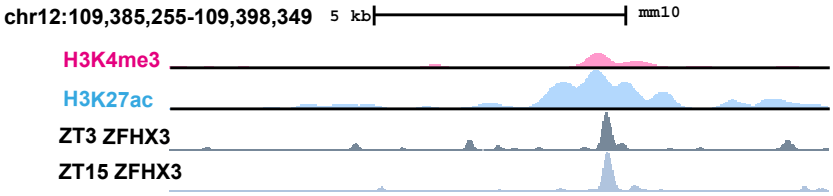

D H3K4me3+ZFHX3

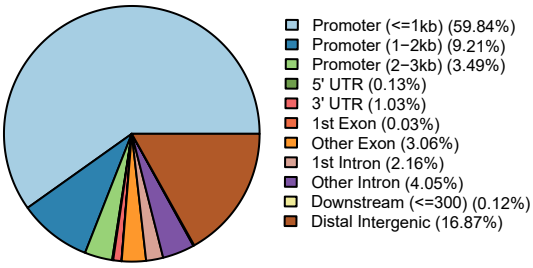

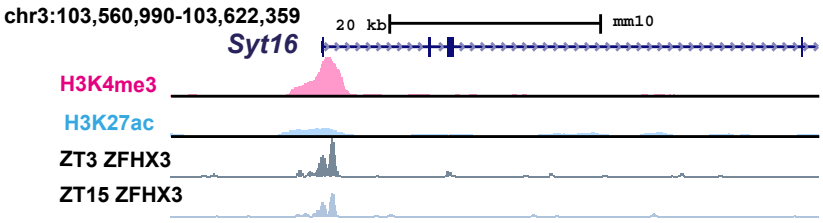

E ZFHX3 ONLY

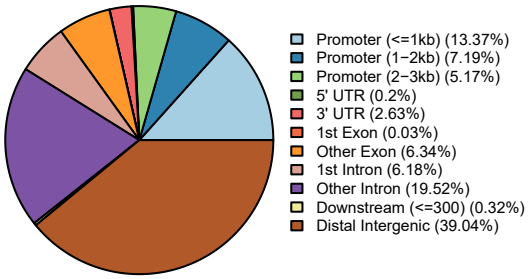

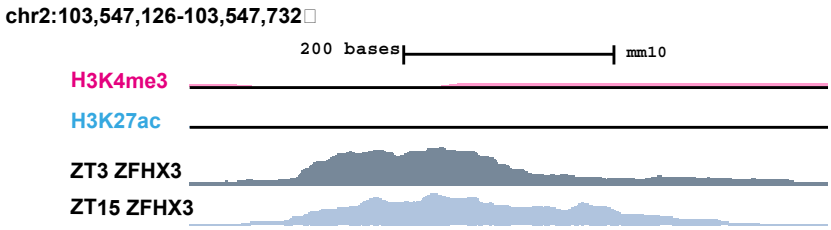

Figure 1. Genomic occupancy of ZFHX3 in the SCN. (A) left- Venn-diagram illustrating overlap of ZFHX3 peaks with histone marks, H3K4me3 and H3K27ac, right- table showing number of sites co-occupied by ZFHX3 and histone marks. (B,C,D and E) left- Genomic feature distribution of ZFHX3 peaks with histone marks (ChIPSeeker), right- UCSC genome browser tracks showing histone modifications H3K4me3(pink), H3K27ac (blue) and ZFHX3 (ZT3 = dark grey and ZT15 = light grey) normalized ChIP-seq read coverage at representative examples for each category. The chromosome location and scale (mm10 genome) indicated at the top.

Figure 2

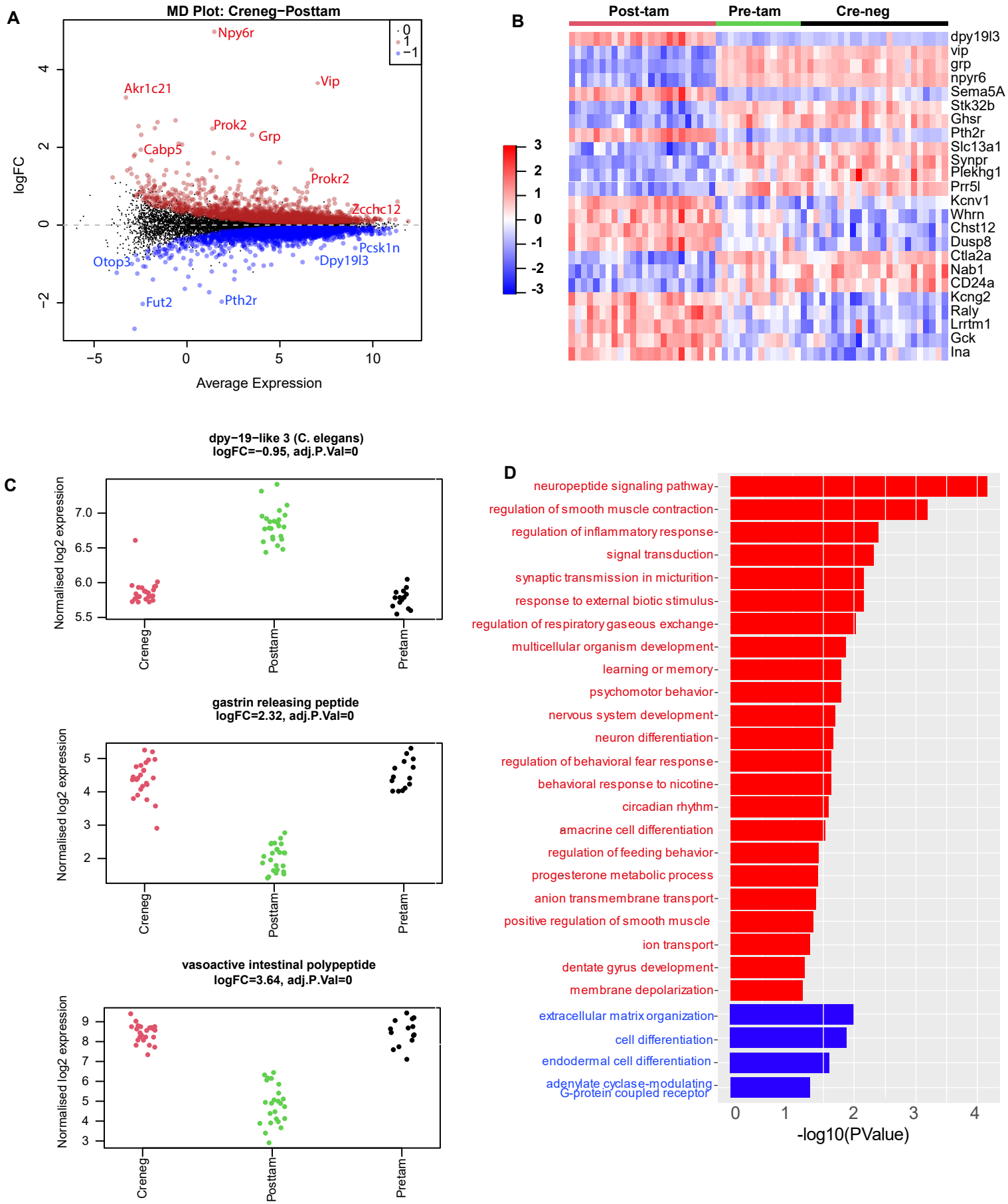

Figure 2. Effect of ZFHX3-KO on SCN transcriptome. (A) Mean-difference plot (MD-plot) showing downregulated (red) and upregulated (blue) gene expression after the loss of ZFHX3. (B) Heatmap showing normalized expression of top 25 (by adj pvalue) differential genes for the compared groups. (C) Stripcharts of differentially expressed genes (*Dpy19l13, Grp, Vip*). (D) Functional annotation of downregulated (red) and upregulated (blue) genes after ZFHX3-KO using the GO::BP (biological processes) terms by DAVID.

Figure 3

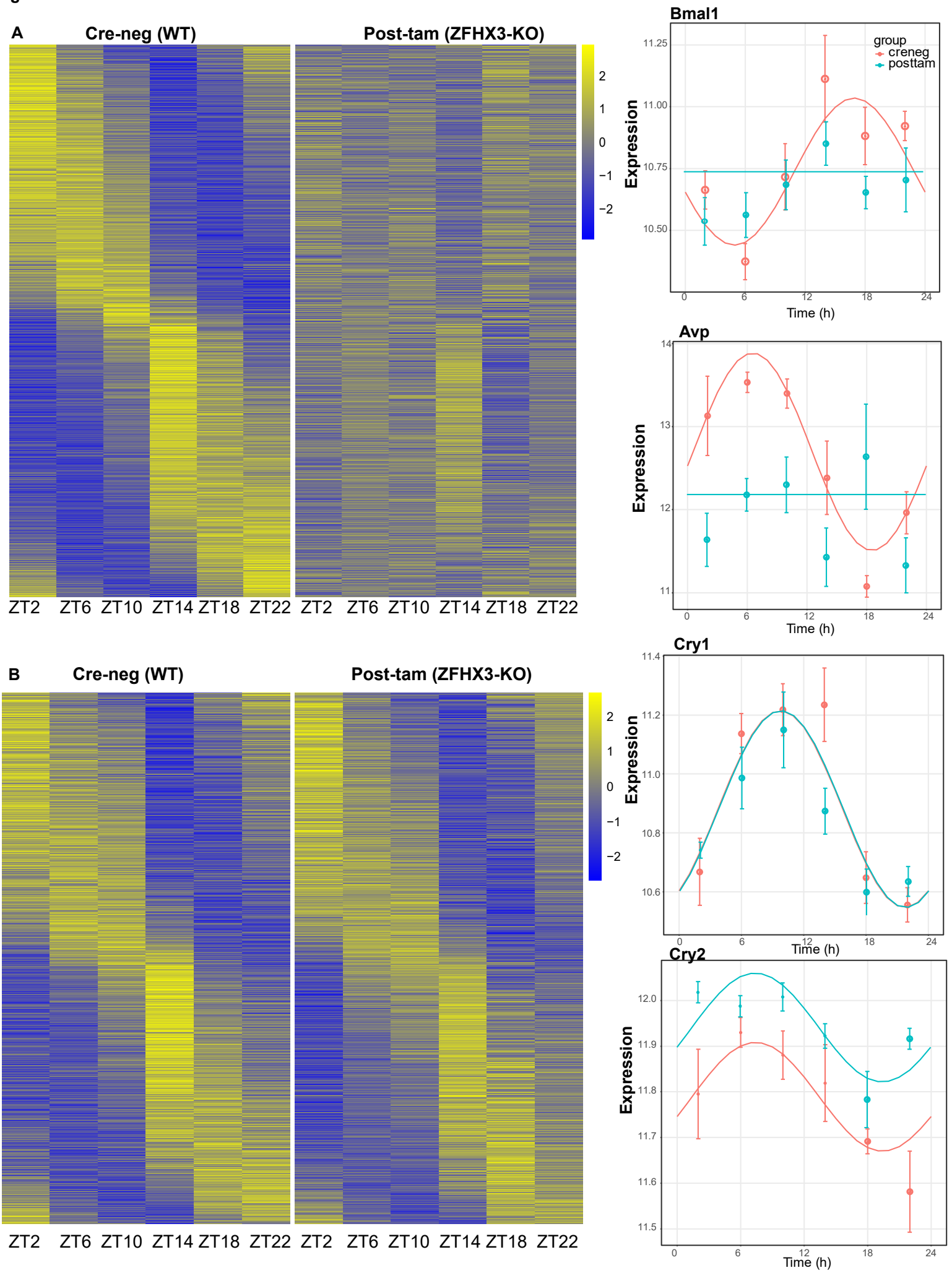

Figure 3. Effect of ZFHX3-KO on rhythmic gene expression . (A) Left- Heatmap showing loss of rhythmic gene expression after *Zfhx3-KO* (module 2) as computed by dryR statistical framework , Right- Illustrative examples of daily abundance of module 2 genes, *Bmal1 and Avp,* in cre-neg and post-tam conditions. (B) Left- Heatmap showing no effect on rhythmic gene expression after *Zfhx3-KO* (module 4) , Right- Illustrative examples of module 4 genes, *Cry1 and Cry2,* in cre-neg and post-tam conditions.